Ablation of Al2O3f/Al2O3 Composites Under Oxyacetylene Torch Flame

Xiang Yang (shmily_0427@163.com)
National University of Defence Technology https://orcid.org/0000-0003-0949-4759
Zhang Wen
NUDT: National University of Defense Technology
Zhu Cheng xin
NUDT: National University of Defense Technology
Wang Yi
Beijing
Peng Zhi hang
NUDT: National University of Defense Technology
Chen Xiao na
Beijing
Ma Yin wei
Beijing
Cao Feng
NUDT: National University of Defense Technology

Research Article

Keywords: Al2O3f/Al2O3 composites, Ablation behavior, Morphology

Posted Date: April 3rd, 2021

DOI: https://doi.org/10.21203/rs.3.rs-376938/v1

Abstract

Continuous alumina fibers reinforced alumina matrix composites (Al_2O_{3f}/Al_2O_3 composites) were produced by following the sol-gel process effectively, while the ablation behavior was analyzed and compared by means of oxyacetylene torch flame test. The results suggested that Al_2O_{3f}/Al_2O_3 composites showed excellent ablation resistance, but no obvious cracks, pits or holes after ablation. The mass and thickness of the sample were barely changed after ablation. After ablation for 120s at 1800℃, the surface morphology of composite material showed no significant change. With the increase of ablation temperature, there were visible signs of high-temperature and high-pressure gas erosion found on the surface of composites. Then, the molten black material began to appear on the surface, and the delamination phenomenon occurred finally. After ablation at 2200℃, the surface of composites became uneven, manifesting large-scale black molten particles, and the area affected by ablation was increasing obvious.

Highlights

1. Al_2O_{3f}/Al_2O_3 composites were fabricated by sol-gel process.
2. Al_2O_{3f}/Al_2O_3 composites showed excellent ablation resistance.
3. The ablation behavior of Al_2O_{3f}/Al_2O_3 composites at 1800℃, 2000℃ and 2200℃ were studied and compared.

1. Introduction

Due to the higher strength, higher toughness and better corrosion resistance, continuous fiber reinforced ceramic matrix composites (CFRCMCs) have been favored by the researchers [1–3]. They have the potential to be applied in aerospace, advanced weapons, ships, and nuclear energy [2–9].

For long-time use under high-temperature environment, the application of non-oxide ceramic matrix composites is severely limited as the fibers and matrix are particularly prone to oxidation and failure [10–12].

As an important branch of CFRCMCs, Oxide/Oxide composites (OCMCs) have attracted more attention with the development of oxide fibers. Oxide ceramics demonstrate excellent corrosion resistance, which makes it suitable for long-time use in high-temperature oxidation environment [12–15].

The Oxide fibers can be divided into the following categories: quartz fibers (SiO_2), aluminosilicate (AS) fibers and alumina fibers (Al_2O_3). Al_2O_3 fibers exhibit better creep resistance and high-temperature resistance behavior [16–21].

The oxide matrix mainly includes silica matrix, mullite matrix and alumina matrix. Among them, alumina matrix shows excellent corrosion resistance. Thus, Al_2O_{3f} /Al_2O_3 composites are expected to be applied

as an alternative material in high-temperature environment [22, 23].

In our previous study, Al_2O_{3f}/Al_2O_3 composites were produced using sol-gel method [23]. The microstructure of Al_2O_3 fibers and Al_2O_3 matrix were examined, while the mechanical properties of Al_2O_{3f} /Al_2O_3 composites were characterized.

Before the practical application of Al_2O_{3f} /Al_2O_3 composites under the high-temperature environment, it is necessary to investigate the evolution of microstructure during ablation. Oxyacetylene torch flame ablation method is the simplest and easiest way to achieve this goal with the minimum cost [24]. However, the studies on ablation morphology and microstructure of Al_2O_{3f} /Al_2O_3 composites have been rarely reported.

In this study, the ablation behavior of Al_2O_{3f}/Al_2O_3 composites was revealed and discussed. Besides, the surface variations of Al_2O_{3f}/Al_2O_3 composites were clarified and compared.

2. Experiments And Methods

2.1 Preparing of Al_2O_{3f}/Al_2O_3 composites

Preparing of Al_2O_{3f}/Al_2O_3 composites: Al_2O_{3f}/Al_2O_3 composites were prepared using sol-gel method [23]. The sol–gel process is detailed as follows: (1) Infiltration, Al_2O_3 fiber preforms were impregnated fully with Al_2O_3 sol (Snowchemical S&T Co., Ltd, China) for about 6 h. (2) Gelation, the fabrics were dried at 200°C for 6 h until gelation. (3) Sintering, the dried Al_2O_3 preforms were sintered at 900°C for 1 h in air. To produce the dense Al_2O_{3f}/Al_2O_3 composites, the sol–gel process was repeated for 12 cycles. The size of the final sample is 30×30×3mm.

2.2 Tests and Characterization

Ablation tests: The ablation behavior of Al_2O_{3f}/Al_2O_3 composites was tested using an oxyacetylene torch (GJB323A-96), and the oxyacetylene flame was parallel to the axial orientation of samples. The ablation resistance test conducted on the Al_2O_{3f}/Al_2O_3 composites is detailed as follows: 1) the ablation performance of the composites was evaluated by oxyacetylene ablation system, with the flow rate and pressure of O_2 set to 850L/h and 0.095MPa respectively, and the flow rate and pressure of C_2H_2 set to 400L/ h and 0.4MPa respectively; 2) the surface temperature of the samples was adjusted by controlling the distance between the flame nozzle and the sample to be tested, with the distance set to the range of 25 ~ 50mm. The temperature should be 1800 ~ 2200℃, and the surface temperature of the sample during ablation should be detected by two-color infrared thermometer; 3) the ablation time was set to 120s. The linear and mass ablation rates of the samples could be obtained according to the formulas below:

$$R_l = \frac{\Delta d}{t} \quad (1)$$

$$R_m = \frac{\Delta m}{t} \quad (2)$$

R_l represents the linear ablation rate, Δd indicates the thickness change of the samples at center region before and after ablation, R_m denotes the mass ablation rate, Δm refers to the mass change of the samples before and after ablation, and t means the ablation time.

Characterization

The microstructure and morphology were analyzed through a combination of field emission scanning electron microscopy (SEM, JSM-5600LV) and energy dispersive spectroscopy (EDS).

The phase composition was investigated by XRD on a Bruker Advanced D8 diffractometer with Cu Kα radiation (λ = 1.5418 Å).

3. Results

3.1 Ablation behavior of Al_2O_{3f}/Al_2O_3 composites

Figure 1 shows the macromorphology of Al_2O_{3f}/Al_2O_3 composites after ablation for 120s at 1800℃, 2000℃ and 2200℃. As shown in Fig. 1, after ablation for 120s at 1800℃, the surface morphology of composite material exhibited no significant change. With the increase of ablation temperature, there were visible signs of high temperature and high pressure gas erosion spotted on the surface of composites, and the molten black material began to appear on the surface. Then, delamination occurred.

After ablation at 2200 ℃, the surface of composites became uneven, large-scale black molten particles appeared, and the area affected by ablation expanded obviously. The reasons for the black surface of the composite material to be observed after ablation are explained as follows. A small amount of Fe_2O_3 in the fiber got oxidized to Fe_3O_4 in the air environment, so that the color was black. Mixed with the molten alumina matrix, the surface of the composite material was shown to be black after ablation.

All samples had no obvious cracks, pits or holes after ablation, and the original flat shape was maintained. The composite had structural integrity and reliability to some extent, suggesting that the ablation resistance of Al_2O_{3f}/Al_2O_3 composites was better.

3.2 XRD of Al_2O_{3f}/Al_2O_3 composites

Figure 2 shows the XRD curves of the composites before and after ablation. The surface of melting particles after ablation at 2200℃ for 120s was taken as ablation products and compared against the

samples without ablation. It can be seen from Fig. 2 that the composition and the composites remained unchanged after ablation, and they were all α-Al_2O_3. The only difference is that the diffraction peak intensity of the ablated product increases significantly, which is attributed to the grain growth of the matrix and fibers at high temperatures during ablation. The results suggested that the microstructure of the composite was stable after high-temperature ablation. Since the fiber and matrix were both high purity alumina, no other chemical reactions occurred, thus ensuring the integrity of the composites.

3.3 The linear and mass ablation rates of Al_2O_{3f}/Al_2O_3 composites

Table 1 shows the ablation performance of Al_2O_{3f}/Al_2O_3 composites after ablation at 1800℃, 2000℃ and 2200℃ for 120s, respectively. Since the mass and thickness of the sample were barely change after ablation at 1800℃, it is discounted here. According to Table 1, the linear ablation rate and mass ablation rate of the composite were extremely low after ablation at 2000℃ and 2200℃ for 120s, indicating that the composites were less affected by ablation. The low linear ablation rate of Al_2O_{3f}/Al_2O_3 composites was closely related to the high melting point of the material. The theoretical melting point of Al_2O_3 was 2054℃. The temperature of this ablation test was close to its melting point, as a result of which the linear ablation rate of the material was low. The mass ablation rate of Al_2O_{3f}/Al_2O_3 composites was mainly related to the viscosity of the material, and the material began to melt after a certain amount of heat was accumulated in the ablation process. While the molten matrix and fiber would be continuously washed by the gas flow with high temperature and pressure, from the center of the sample to the edge of the sample. Due to the high viscosity of alumina at high temperatures, it was difficult to remove by the gas flow, but stayed on the surface of the composites. After cooling, the molten particles were formed, so that the mass loss of the composite material was insignificant, and the mass ablation rate was also very low. The lower linear ablation rate and mass ablation rate indicated that Al_2O_{3f}/Al_2O_3 composites had strong ablation resistance.

Table 1
The ablation performance of Al_2O_{3f}/Al_2O_3 composites after ablation

Properties	**Al_2O_{3f}/Al_2O_3 composites**		
Ablation time/s	120		
Ablation temperature/℃	1800	2000	2200
Linear ablation rate/mm/s	—	0.00167	0.00321
weight ablation rate/g/s	—	0.00097	0.00156

3.4 Morphology of Al_2O_{3f}/Al_2O_3 composites

Figure 3 shows the original surface and cross-section morphology of the composites. It could be seen from Fig. 3 that the surface of the composites was a layer of alumina, and that its surface was roughly flat, with undulations and cracks observed. The cracks were mainly caused by the thermal stress generated in the sintering process of the matrix. It could be seen from the cross-section of the composite that the interior of the composites was relatively compact, the fiber and the matrix were bonded well, and there were no obvious pores or defects. The continuity and integrity of the composites suggested better mechanical properties and stronger ablation resistance.

Figure 4 shows the microstructure and EDS analysis of the composites after ablation at 2200℃ for 120s. According to EDS analysis, there were only two elements Al and O in A, B and C. Based on the proportion of these elements, it could be inferred that the phase composition of the composite surface remained unchanged after ablation, which means it remained Al_2O_3. It could be seen from Fig. 4 that the ablated surface of the composite could be roughly divided into three areas. Firstly, at point A, the edge of the samples was a continuous layer of Al_2O_3 matrix, which was less affected by the ablation. This is mainly because the matrix became more compact and compact after heat treatment, and the surface was smoother. Secondly, at point B, most of the matrix in the composites was washed away by the air flow at high temperatures, thus leading to a lot of defects Al_2O_3 fibers. Besides, the structure and braiding of the fibers were also affected, belonging to the ablation transition region. Lastly, at point C, the ablation center of the sample had the highest temperature in the ablation process, and the fibers melted at high temperatures, thus forming many small segments of structure. Mixed with the fused alumina matrix, they were deposited at the edge of the ablation center, cooled and solidified. The mixture of fiber and matrix was formed after the treatment.

Figure 5 shows the cross-section micro morphology of Al_2O_{3f}/Al_2O_3 composites after ablation at 2200℃ for 120s. It can be seen from Fig. 5 that the cross-section morphology of the composites was mainly divided into two areas: 1) zone I, the reaction area in the ablation process. The average thickness of the whole reaction area was about 250μm. In this area, there were plenty of pores in the composites, and the whole appearance was starkly different than in zone II. There was no clear fiber braiding pattern observed, and the structure of the composites suffered damage. According to the locally enlarged view of point A, this area was mainly comprised of fused fiber and alumina matrix, and the continuous toughened fiber in this area was fused at high temperatures and mixed with the molten alumina matrix; 2) zone II, the unaffected area in the ablation process, in which the composite was basically unaffected by ablation and remained stable. The original structure and morphology of the composites were observed.

4. Conclusions

Al_2O_{3f}/Al_2O_3 composites were produced by sol-gel effectively. The ablation behavior of Al_2O_{3f}/Al_2O_3 composites was tested. The results were summarized as follows:

(1) Al_2O_{3f}/Al_2O_3 composites had excellent ablation resistance. All samples showed no obvious cracks, pits or holes after ablation, and the original flat shape was maintained.

(2) After ablation for 120s at 1800℃, the surface morphology showed no significant change. The mass and thickness of the sample were barely changed after ablation.

(3) After ablation at 2200℃, the surface of composites became uneven, large-scale black molten particles appeared, and the area affected by ablation expanded significantly.

Declarations

Acknowledgements

The authors are grateful to Hunan Natural Science Foundation (2020JJ5660) and Key Laboratory Fund (6142907180402) for financial support. The authors are also grateful to Aid Program for Innovative Group of National University of Defense Technology and Aid Program for Science and Technology Innovative Research Team in Higher Educational Institutions of Hunan Province.

Conflict of Interest Statement:

The enclosed is a paper, entitled "**Ablation of Al_2O_{3f}/Al_2O_3 composites under oxyacetylene torch flame**". Please accept it as a candidate for published. The follows are my responses to your submission requirements.

To the best of our knowledge, the productions of this paper are original. All authors have read the paper and agree to this statement of originality. Finally, this paper is our original unpublished work and it has not been submitted to any other journal for reviews. The authors have obtained the necessary authority for publication. If accepted, this paper will not be published elsewhere in the same form, in English or in any other language, without the written consent of the Publisher.

References

1. Armani CJ, Ruggles-Wrenn MB, Hay RS et al (2013) Creep and microstructure of NextelTM720 fiber at elevated temperature in air and in steam. Acta Mater 61(16):3114–3124
2. Chen X, Cheng G, Zhang J et al. Residual stress variation in SiCf/SiC composite during heat treatment and its effects on mechanical behavior[J]. Journal of Advanced Ceramics.2020, 9(5): 567–575
3. Yang X, Wei L, Song W et al (2012) Oxidation behavior of oxidation protective coatings for PIP-C/SiC composites at 1500°C. Ceram Int 38:9–13
4. Xiang Y, Wang Q, Peng ZH, Cao F (2016) High-temperature properties of 2.5D SiO2f/SiO2 composites by sol–gel. Ceram Int 42:12802–12806

5. Liu G, Zhang X, Yang J, et al (2019) Recent advances in joining of SiC-based materials (monolithic SiC and SiCf/SiC composites): Joining processes, joint strength, and interfacial behavior[J]. Journal of Advanced Ceramics 8(01):21–40
6. Yang X, Lu-ming H (2014) C. Zhao-hui. Degradation of CVD-SiC coated PIP-C/SiC composites exposed to the hot firing test based on MMH/N2O4 bipropellants. Ceram Int 40:10303–10308
7. Wang Q, Cao F, Xiang Y et al (2017) Effects of ZrO_2 coating on the strength improvement of 2.5D SiC_f/SiO_2 composites. Ceram Int 43:884–889
8. Yu Z, Wang SB (2011) Synthesis of boron nitride coatings on quartz fibers: thickness control and mechanism research. Appl Surf Sci 257:10752–10757
9. Yang X, Qing W, Feng C et al (2017) Sol-gel process and high-temperature property of SiO_2/ZrO_2-SiO_2 composites. Ceram Int 43:854 ~ 859
10. Nasrin N, Niranjan P et al (2016) Oxidation behaviour of SiC/SiC ceramic matrix composites in air. J Eur Ceram Soc 36:3293–3302
11. Zhuang L, Fu QG et al (2018) Oxidation protection of C/C composites: coating development with thermally stabile SiC/PyC nanowires and an interlocking TaB2-SiC structure. Corros Sci 26:2366–2373
12. Wang J, Yang Z, Duan X, et al (2015) Microstructure and mechanical properties of SiCf/SiBCN ceramic matrix composites[J]. Journal of Advanced Ceramics 4(1):31–38
13. Zhang Y, Chen J, Fan H et al (2015) Characterization of modified SiC@SiO2 nanocables/ MnO2 and their potential application as hybrid electrodes for super capacitors. Dalton Trans: Int J Integr Care 44(46):19974–19982
14. Chawla KK (2008) Interface engineering in mullite fiber/mullite matrix composites. J Eur Ceram Soc 28:447–453
15. Zhu CX, Cao F, Xiang Yang Y et al., Thermal shock resistance of Al_2O_3/SiO_2 composites by sol-gel. Ceram. Int. https://doi.org/10.1016/j.ceramint.2019.02.201
16. Ruggles-Wrenn MB, Musil SS, Mall S et al (2006) Creep behavior of NextelTM610/ monazite/alumina composites at elevated temperatures. Compos Sci Technol 66:2089–2099
17. Wang Y, Cheng HF, Liu HT, Zu M, Wang J (2013) Microstructure and room temperature mechanical properties of mullite fibers after heat-treatment at elevated temperatures. Mater Sci Eng 578:287–293
18. Marina B, Ruggles W (2018) Mechanical Behavior of Oxide–Oxide Fiber-Reinforced CMCs at Elevated Temperature: Environmental Effects. Comprehensive Composite Materials 5:174–236
19. Volkmann E, Tushtev K et al (2015) Assessment of three oxide/oxide ceramic matrix composites: Mechanical performance and effects of heat treatments. Compos Appl Sci Manuf 68:19–28
20. Parlier M, Ritti MH (2003) State of the art and perspectives for oxide/oxide composites. Aero Sci Technol 7:211–221

21. Wang Y, Cheng HF, Liu HT et al (2015) Corrosion behavior of pyrocarbon coatings exposed to Al_2O_3-SiO_2 gels containing ammonium nitrate. Corros Sci 94:401–410
22. Ramdane CB, Julian-Jankowiak A, Valle R et al (2017) Microstructure and mechanical behaviour of a Nextel™610/alumina weak matrix composite subjected to tensile and compressive loadings. J Eur Ceram Soc 37:2919–2932
23. Chengxin Z, Feng C, Yang X et al., Effects of sintering temperature on mechanical properties of alumina fiber reinforced alumina matrix composites, Journal of Sol-Gel Science and Technology. https://doi.org/10.1007/s10971-019-05192-z
24. Yang X, Wei L, Song W et al (2013) ZrB2/SiC as a protective coating for C/SiC Composites: effect of high temperature oxidation on mechanical properties and anti-ablation property. Composites Part B 45:1391–1396

Figures

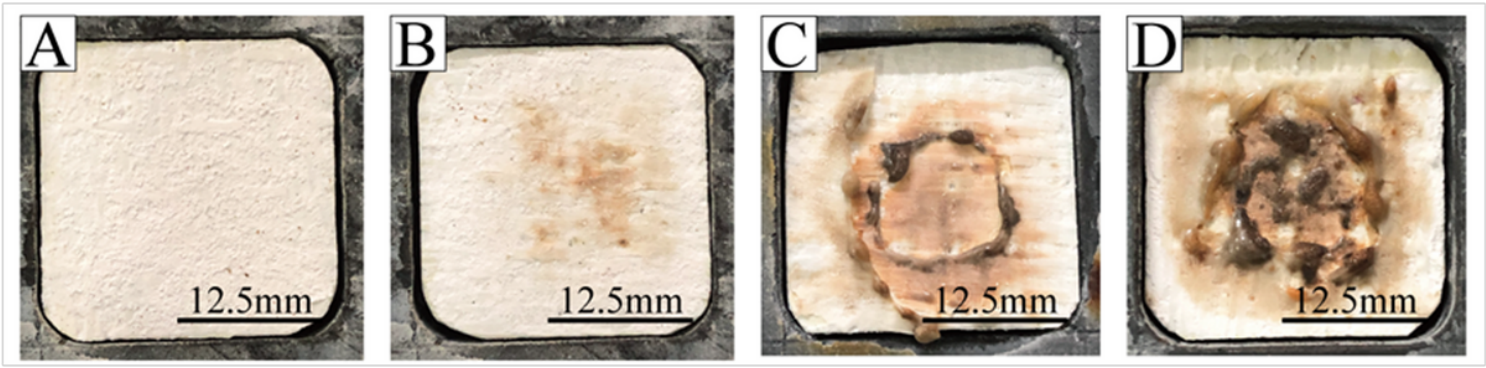

Figure 1

The macromorphology of Al2O3f/Al2O3 composites after ablation for 120s at 1800℃, 2000℃ and 2200℃

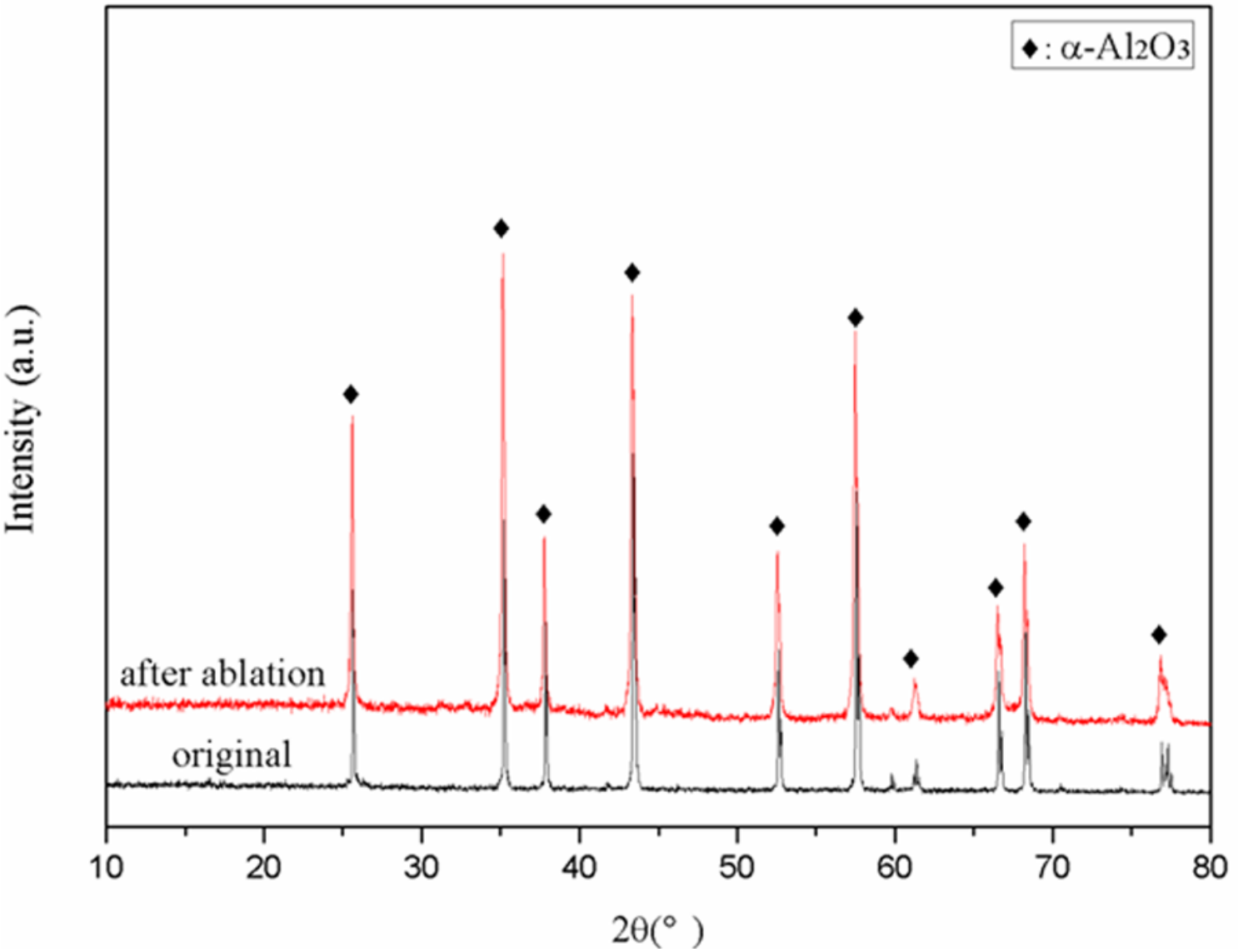

Figure 2

The XRD curves of the composites before and after ablation

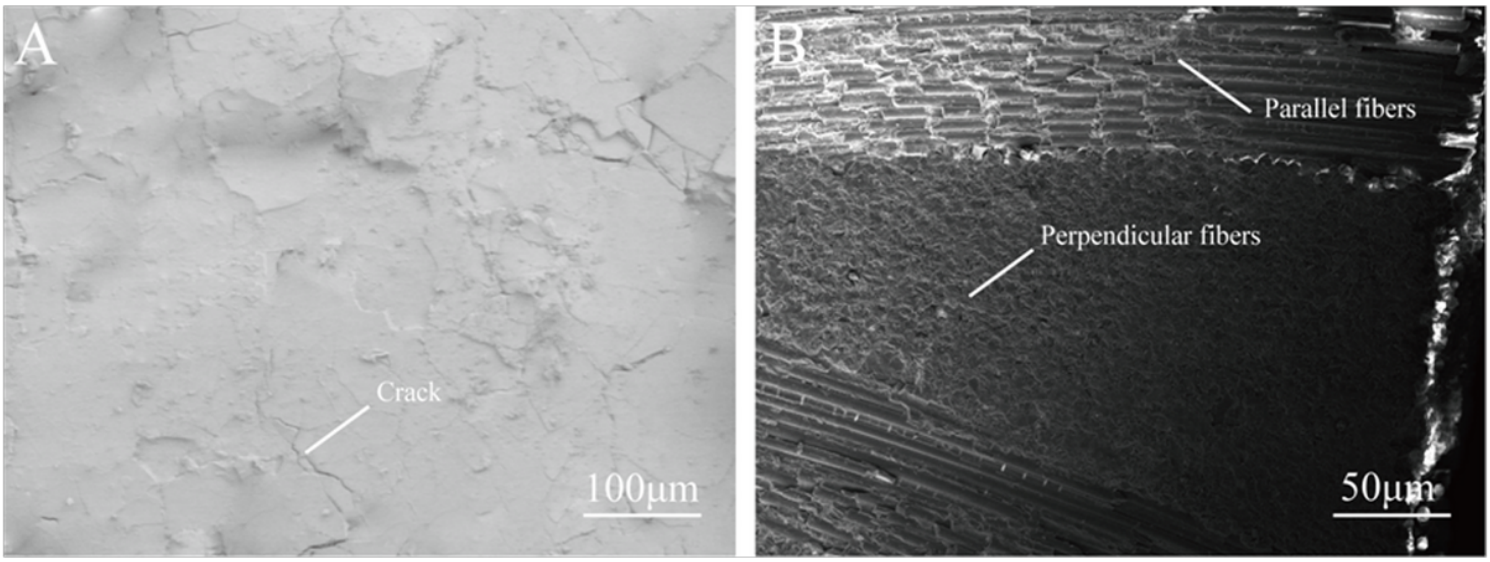

Figure 3

The original surface and cross-section morphology of the composites

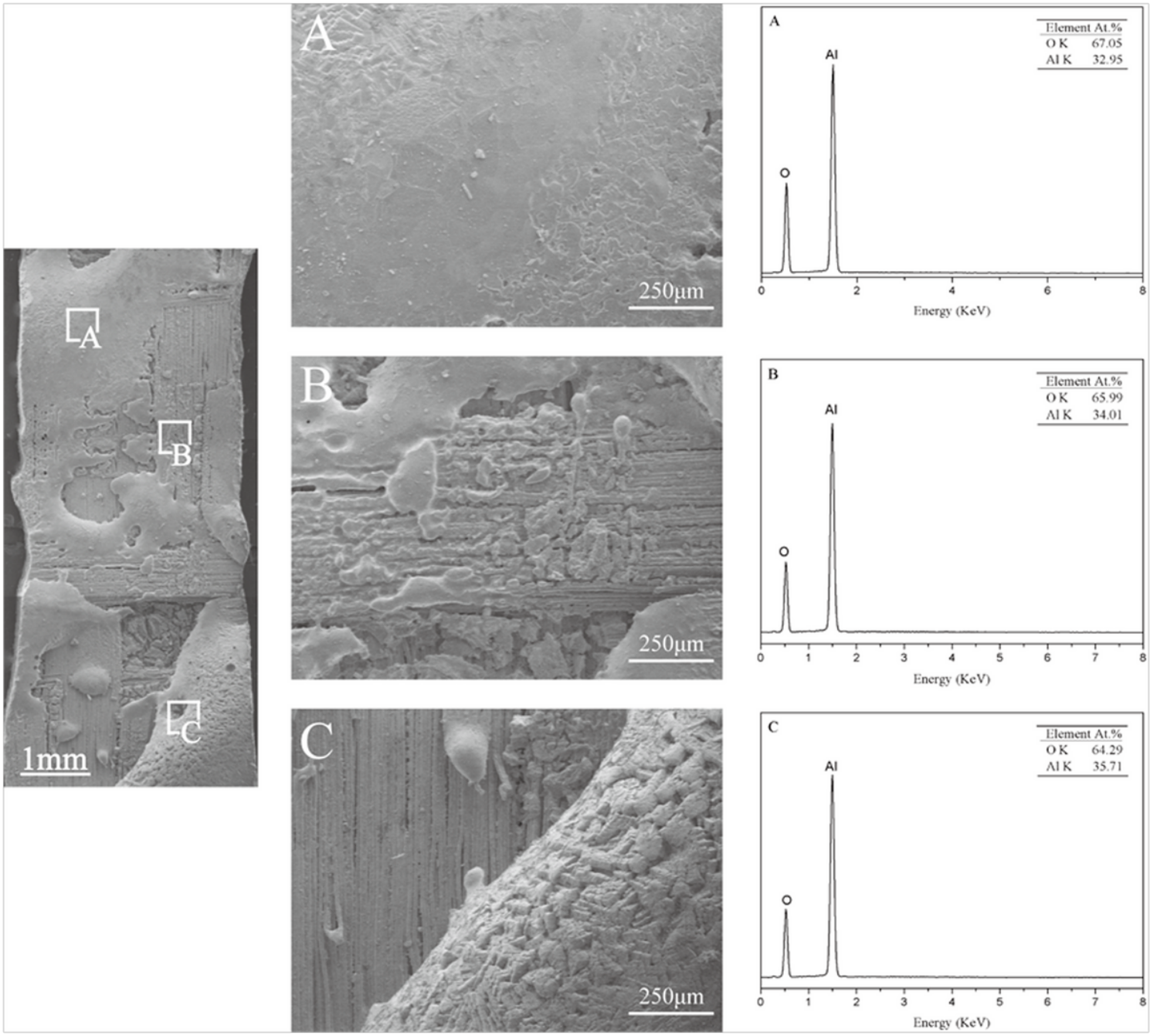

Figure 4

The microstructure and EDS analysis of the composites after ablation at 2200°C for 120s

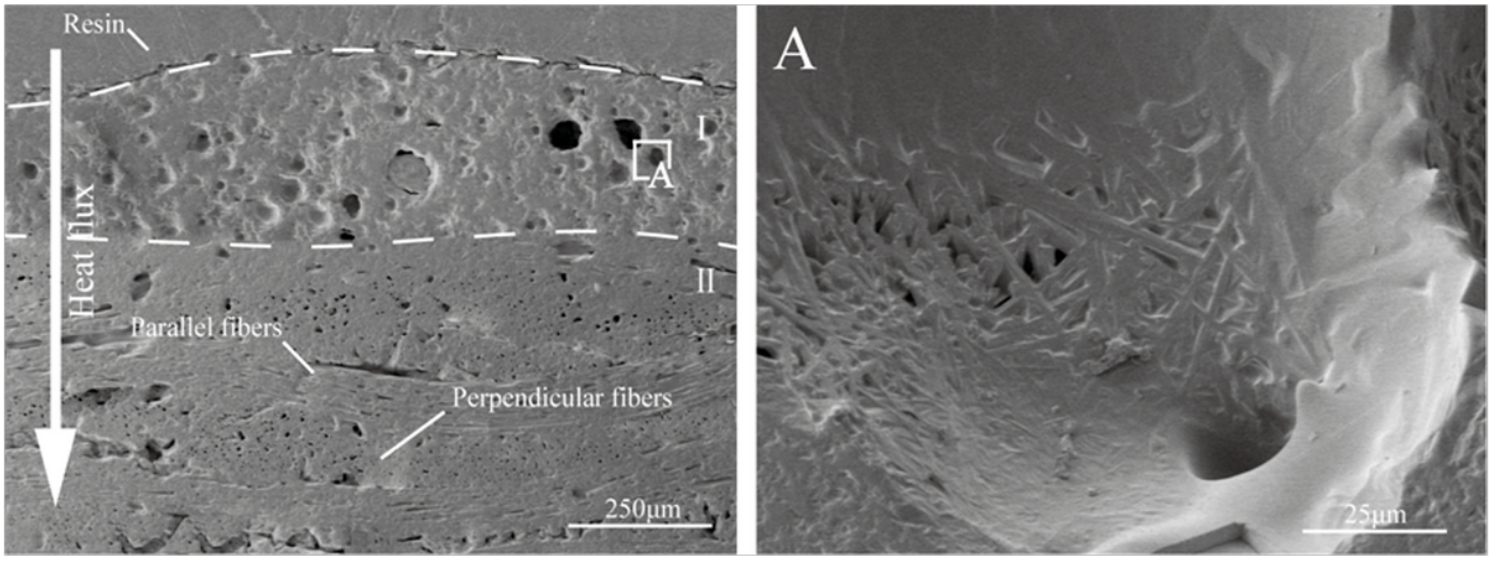

Figure 5

The cross-section micro morphology of Al2O3f/Al2O3 composites after ablation at 2200℃ for 120s